A&A 496, 399–412 (2009)
DOI: 10.1051/0004-6361/200811029

Astronomy & Astrophysics

Depth estimation of the Large and Small Magellanic Clouds

S. Subramanian and A. Subramaniam

Indian Institute of Astrophysics, Bangalore, India
e-mail: [smitha;purni]@iiap.res.in

Received 24 September 2008 / Accepted 15 December 2008

ABSTRACT

Context. A systematic estimation of the line of sight depth in the disk and bar regions of the Large and Small Magellanic Clouds (LMC and SMC) using red clump stars is presented.
Aims. We used the red clump stars from the photometric data of the Optical Gravitational Lensing Experiment (OGLE II) survey and the Magellanic Cloud Photometric Survey (MCPS) for both the Clouds to estimate the depth.
Methods. The observed dispersion in the magnitude and colour distribution of red clump stars is used to estimate the depth, after correcting for population effects, internal reddening within the Clouds and photometric errors.
Results. The observed dispersion due to the line of sight depth ranges from 0.023 mag, to 0.45 mag (a depth of 500 pc to 10.4 kpc) for the LMC and, from 0.025 to 0.34 mag (a depth of 670 pc to 9.53 kpc) for the SMC. The minimum value corresponds to the dispersion that can be estimated due to errors. The depth profile of the LMC bar indicates that it is flared. The average depth in the bar region is 4.0 ± 1.4 kpc. The northern disk is found to have depth (4.17 ± 0.97 kpc) larger than the southern part of the disk (2.63 ± 0.8 kpc). There is no indication of depth variation between the eastern (2.8 ± 0.92 kpc) and the western (3.09 ± 0.99 kpc) disk. The average depth for the disk is 3.44 ± 1.16 kpc. The SMC is found to have larger depth than the LMC. In the case of the SMC, the bar depth (4.90 ± 1.23 kpc) and the disk depth (4.23 ± 1.48 kpc) are found to be within the standard deviations. A prominent feature in the SMC is the increase in depth near the optical center. The averaged depth profile near the center resembles a structure like a bulge.
Conclusions. The large dispersions estimated in the LMC bar and the northern disk suggest that the LMC either has large depth and/or different stellar population in these regions. The halo of the LMC (using RR Lyrae stars) is found to have larger depth compared to the disk/bar, which supports the existence of an inner halo for the LMC. On the other hand, the estimated depths for the halo (RR Lyrae stars) and disk are found to be similar, for the SMC bar region. Thus, increased depth and enhanced stellar as well as HI density near the optical center suggests that the SMC may have a bulge.

Key words. stars: horizontal-branch – galaxies: Magellanic Clouds – galaxies: halos – galaxies: stellar content – galaxies: structure – galaxies: bulges

1. Introduction

The Large Magellanic Cloud (LMC) and Small Magellanic Cloud (SMC) are nearby irregular galaxies at a distance of about 50 kpc and 60 kpc respectively. Both these galaxies are nearly face on. Magellanic Clouds (MCs) were believed to have had interactions with our Galaxy as well as between each other (Westerlund 1997). It is also believed that the tidal forces due to these interactions have caused structural changes in these galaxies. The recent proper motion estimates by Kallivayalil et al. (2006a,b) and Besla et al (2007) indicate that these Clouds may be approaching our Galaxy for the first time. These results also claim that the MCs might not have always been a binary system. Therefore, it is not clear whether the structure of the MCs is modified due to their mutual interactions, interactions with our Galaxy or something else, like minor merges.

The *N*-body simulations by Weinberg (2000) predicted that the LMC's evolution is significantly affected by its interactions with the Milky Way, and the tidal forces will thicken and warp the LMC disk. Alves & Nelson (2000) studied the carbon star kinematics and found that the scale height, h, increased from 0.3 to 1.6 kpc over the range of radial distance, R, 0.5 to 5.6 kpc and hence concluded that the LMC disk is flared. Using an expanded sample of carbon stars, van der Marel et al. (2002) also found that the thickness of the LMC disk increases with the radius. The depth of the clouds could vary as a function of radial distance from the center due to tidal forces. The presence of variation in depth across the LMC, if present, is likely to give valuable clues to the interactions it has experienced in the past. There has not been any direct estimate of the thickness or the line of sight depth of the bar and disk of the LMC so far.

Mathewson et al. (1986, 1988) found that SMC cepheids extend from 43 to 75 kpc with most cepheids found in the neighbourhood of 59 kpc. Later, the line of sight depth of SMC was estimated (Welch 1987) by investigating the line of sight distribution and period – luminosity relation of cepheids. They accounted for various factors which could contribute to the larger depth estimated by Mathewson et al. (1986, 1988), and found the line of sight depth of the SMC to be ∼3.3 kpc. Hatzidimitriou et al. (1989), estimated the line of sight depth in the outer regions of the SMC to be around 10–20 kpc.

Red Clump (RC) stars are core helium burning stars, which are metal rich and slightly more massive counterparts of the horizontal branch stars. They have tightly defined colour and magnitude, and appear as an easily identifiable component in colour magnitude diagrams (CMDs). RC stars were used as standard candles for distance determination by Stanek et al. (1998). They used the intrinsic luminosity to determine the distance to MCs as well as to the bulge of our Galaxy. Olsen & Salyk (2002) used their constant I band magnitude to show that the southern LMC disk is warped. Subramaniam (2003) used the constant magnitude of RC stars to show that the LMC has some structures and

warps in the bar region. Their characteristic colour was used by Subramaniam (2005) to estimate the reddening map towards the central region of the LMC.

In this paper, we used the dispersions in the colour and magnitude distribution of RC stars for depth estimation. The dispersion in colour is due to a combination of observational error, internal reddening (reddening within the disk of the LMC/SMC) and population effects. The dispersion in magnitude is due to internal disk extinction, depth of the distribution, population effects and photometric errors associated with the observations. By deconvolving other effects from the dispersion of magnitude, we estimated the dispersion only due to the depth of the disk. The advantage of choosing RC stars as a proxy is that there are large numbers of these stars available to determine the dispersions in their distributions with good statistics, throughout the L&SMC disks. The depth estimated here would correspond to the depth of the intermediate age L&SMC disks. The depth of the intermediate age disk of these galaxies may give clues to their formation and evolution, and thus in turn would give clues to their mutual interactions. This could also place some constraints on their interaction with our Galaxy. Measurements of line of sight depth in the central regions of MCs, especially the LMC, is of strong interest to understand the observed microlensing towards these galaxies.

The next section deals with the contribution of population effects to the observed dispersion of RC stars. Data sources are explained in Sect. 3 and details of the analysis is described in Sect. 4. Internal reddening in the MCs is explained in Sect. 5. The LMC and SMC results are presented in Sects. 6 and 7 respectively and their implications are discussed in Sect. 8. These results for the disks are compared with the depth estimates of the halo, as defined by RR Lyrae stars, in Sects. 9 and 10. Conclusions are given in Sect. 11.

2. Effect of a heterogeneous population of RC stars

The RC stars in the L&SMC disks are a heterogeneous population and hence, they would have a range in mass, age and metallicity. The density of stars in various location will also vary with the local star formation rate as a function of time. These factors result in a range of magnitude and colour of the net population of RC stars in any given location and would contribute to the observed dispersion in magnitude and colour distributions. Girardi & Salaris (2001) simulated the RC stars in the LMC using the star formation rate estimated by Holtzman et al. (1999) and the age metallicity relation from Pagel & Tautvaisiene (1998). They also simulated the RC stars in SMC using star formation results and the age metallicity relation from Pagel & Tautvaisiene (1998). The synthetic CMDs of the two systems were obtained and the distribution of RC stars is fitted using numerical analysis to obtain the mean and dispersion of the magnitude and colour distributions. The estimated intrinsic dispersions in magnitude and colour distributions for LMC are 0.1 and 0.025 mag respectively. In the case of the SMC, the values are 0.076 and 0.03 mag respectively. The values of colour dispersions are measured from the CMDs given in the above reference. We used these estimates of the intrinsic dispersion, to account for the population effects in our analysis.

The above reference used two models of star formation history, one for the bar and the other for the disk of the LMC. The width of the RC distribution for the above two populations is not very different. They also simulated the RC distribution found by Dolphin (2000) in the northern LMC. The RC stars in this region were found to be very different due to a significantly different star formation history and metallicity. The effect on the width of the RC was found to be large. The intrinsic dispersion in this region was found to be 0.218 mag, double that of the bar population. Therefore, if the population of a region is different, its effect on the width of the RC distribution will be to increase it. All the regions in the bar and the disk were corrected for population effects using the bar and the disk model estimates of width. There may be an uncorrected component due to population effects in the estimated depth, due to variations in the RC population between regions. The final estimated variation of RC width will be a combination of variation in depth and population across the LMC. In the SMC also, there can be an effect of different RC populations in the dispersion corresponding to depth. The contribution of these components in various locations of the MCs will be discussed later.

3. Data

3.1. LMC data

The OGLE II survey (Udalski et al. 2000; Szymanski 2005; Udalski et al. 1997) scanned the central region of the LMC to detect microlensing events. One of the outcomes of this survey is a catalogue of stars in the central/bar region of the LMC, consisting of photometric data of 7 million stars in the B, V and I pass bands. This catalogue presents data of 26 fields which cover the central 5.7 square degrees of the LMC in the sky. Out of the 26 regions/strips, 21 regions are within 2.5 degrees of the optical center of the LMC representing the bar region, and the other 5 regions are in the north western part of the LMC disk. The average photometric error of red clump stars in I and V bands are ~0.05 mag. Photometric data with errors less than 0.15 mag are considered for the analysis. Each strip was divided into 4×16 smaller regions, each having an area of 3.56×3.56 square arcmin. Thus 26 strips of the LMC were divided into 1664 regions. $(V - I)$ vs. I CMDs were plotted for each region and a sample CMD of one such region is shown in Fig. 1. For all the regions, red clump stars were well within a box in the CMD, with widths 0.65–1.35 mag in $(V - I)$ colour and 17.5–19.5 mag in I magnitude. Thus, the red clump stars were identified in each region. The OGLE II data suffers from incompleteness due to crowding effects and the incompleteness in the RC distribution is corrected using the values given in Udalski et al. (2000).

The Magellanic Cloud Photometric Survey (MCPS, Zaritsky et al. 2004) of the central 64 square degrees of the LMC contains photometric data of around 24 million stars in the U, B, V and I pass bands. Data with errors less than 0.15 mag are taken for the analysis. The regions away from the bar are less dense compared to the bar region. The total observed regions are divided into 1512 sub-regions each having an area of approximately 10.53×15 square arcmin. Out of 1512 regions only 1374 regions have a reasonable number of RC stars to do the analysis. $(V - I)$ vs. I CMDs for each region were plotted and red clump stars were identified as described above.

3.2. SMC data

The OGLE II survey (Udalski et al. 1998) of the central region of the SMC contains photometric data of 2 million stars in the B, V and I pass bands. The catalogue of SMC presents data of 11 fields which cover the central 2.5 square degrees of the SMC in the sky. The observed regions of the SMC are divided into 176 regions. Each strip was divided into 2×8 regions, each

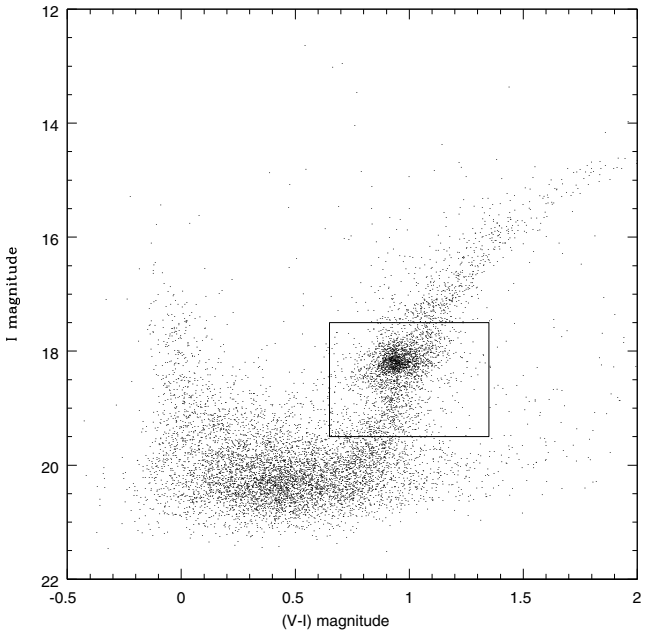

Fig. 1. Colour magnitude diagram of an LMC region. The box used to identify the RC population is shown.

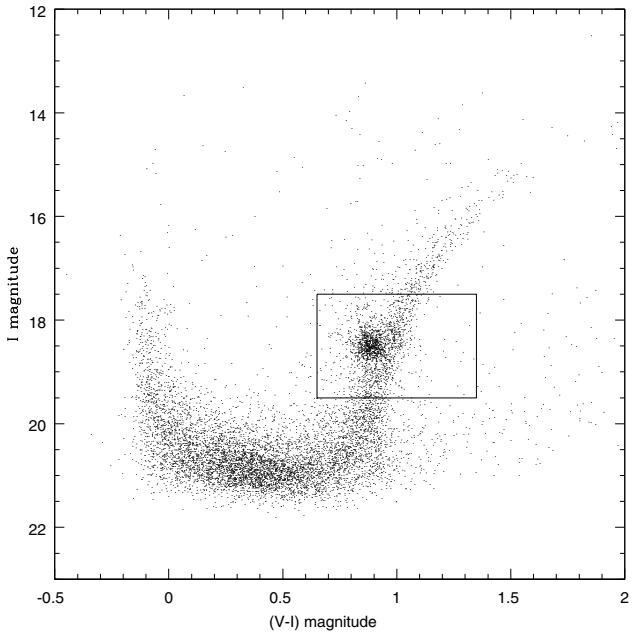

Fig. 2. Colour magnitude diagram of an SMC region. The box used to identify the RC population is shown.

having an area of 7.12 × 7.12 square arcmin to obtain enough stars in each region. Data selection and analysis is similar to that for the LMC, including the box used to identify the RC stars in the CMD. A sample CMD for one location is shown in Fig. 2. We used the incompleteness corrections given in Udalski et al. (1998).

The Magellanic Cloud Photometric Survey (MCPS, Zaritsky et al. 2002) of the central 18 square degrees of the SMC contains photometric data of around 5 million stars in the U, B, V and I pass bands. Data with errors less than 0.15 mag are taken for the analysis. The regions away from the bar are less dense compared to the bar region. The total observed regions are divided into 876 sub-regions each having an area of approximately 8.9×10 square arcmin. Out of 876 regions, 755 regions with a reasonable number of RC stars were considered for analysis.

4. Analysis

A spread in magnitude and colour of red clump stars is observed in the CMDs of both the LMC and SMC. Their number distribution profiles roughly resemble a Gaussian. The width of the Gaussian in the distribution of colour is due to the internal reddening, apart from observational error and population effects. The width in the distribution of magnitude is due to population effects, observational error, internal extinction and depth. By deconvolving the effects of observational error, extinction and population effects from the distribution of magnitude, an estimate of depth can be obtained.

To obtain the number distribution of the red clump stars in each region, the data are binned with a bin size of 0.01 and 0.025 mag in colour and magnitude respectively. The obtained distributions in colour and magnitude are fitted with a function, a Gaussian + quadratic polynomial. The Gaussian represents the red clump stars and the other terms represent the red giants in the region. A non linear least square method is used for fitting and the parameters are obtained. In Figs. 3 and 4, the distribution

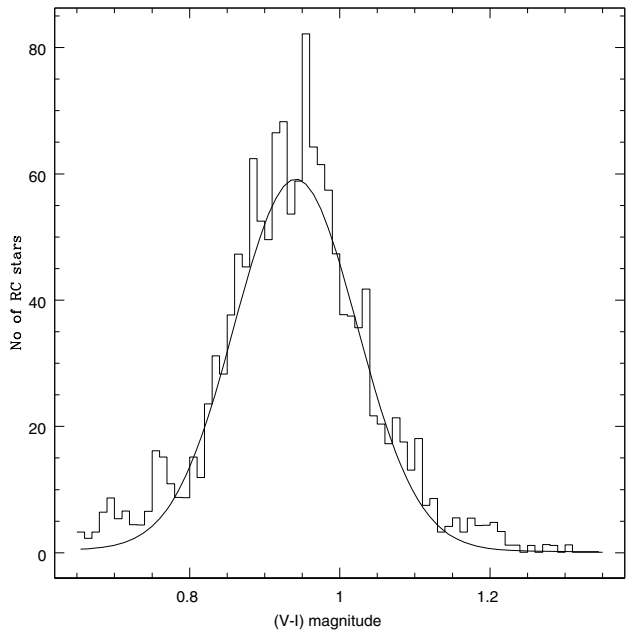

Fig. 3. A typical colour distribution of red clump stars in the LMC. The best fit to the distribution is also shown. The reduced χ^2 value of this fit is 1.33.

as well as the fitted curve are shown for both colour and magnitude distribution of an LMC region (OGLE II data). Similarly for SMC (OGLE II data), the distribution as well as the fitted curve are shown for both colour and magnitude in Figs. 5 and 6. The parameters obtained are the coefficients of each term in the function used to fit the profile, the error in the estimation of each parameter and the goodness of the fit, which is the same as the reduced χ^2 value. Regions with reduced χ^2 values greater than 2.6 are omitted from the analysis. As the important

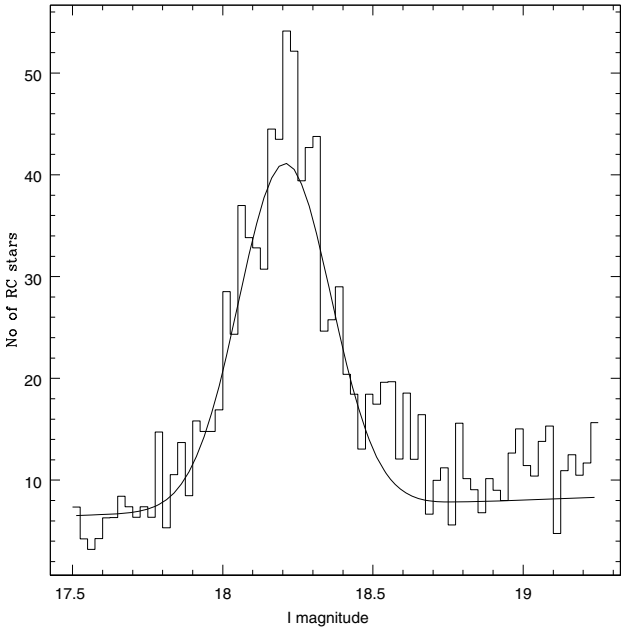

Fig. 4. A typical magnitude distribution of red clump stars in the LMC. The best fit to the distribution is also shown. The reduced χ^2 value of this fit is 0.99.

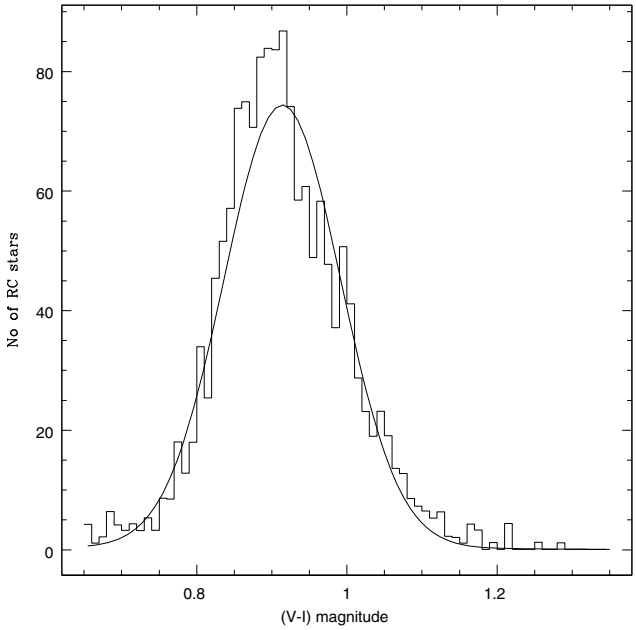

Fig. 5. A typical colour distribution of red clump stars in the SMC. The best fit to the distribution is also shown. The reduced χ^2 value of this fit is 1.18.

parameter for our calculations is the width associated with the two distributions, we also omitted regions with fit errors of width greater than 0.1 mag from our analysis. After these omissions, the number of regions useful for analysis in LMC (OGLE II data) and LMC (MCPS data) is reduced from 1664 to 1528 and from 1374 to 1301 respectively. Similarly for the SMC, after omitting regions with larger reduced χ^2 values and fit error values, the number of regions useful for analysis in OGLE II data and MCPS data is reduced from 176 to 150 and from 755 to 600 respectively. Thus, the total observed dispersion in $(V-I)$ colour and I magnitude were estimated for RC stars in all these regions. The number of RC stars in each region studied in the MCs depends on the RC density. The number is large in the central regions, whereas it decreases in the disk. In LMC, the RC stars range between 500–2000 in the bar region, whereas the range is 200–1500 in the disk. In the central regions of the SMC, the RC stars range between 1000–3000. The disk is found to have a range 200–1500.

The following relations are used to estimate the resultant dispersion due to depth from the above estimated dispersions.

$$\sigma^2_{\rm col} = \sigma^2_{\rm internalreddening} + \sigma^2{}_{\rm intrinsic} + \sigma^2{}_{\rm error}$$

$$\sigma^2{}_{\rm mag} = \sigma^2{}_{\rm depth} + \sigma^2{}_{\rm internalextinction} + \sigma^2{}_{\rm intrinsic} + \sigma^2{}_{\rm error}.$$

The average photometric errors in I and V band magnitudes were calculated for each region and the error in I magnitude and $(V-I)$ colour were estimated. These were subtracted from the observed width of magnitude and colour distribution respectively, thus accounting for the photometric errors (last term in the above equations). The contribution from the heterogeneous population of RC stars were discussed in Sect. 2, and the dispersion in colour and magnitude due to this effect ($\sigma_{\rm intrinsic}$) were also subtracted from the observed dispersions. After correcting for the population effects and the observational error in colour, the remaining spread in colour distribution (first equation) is taken as due to the internal reddening, $E(V-I)$. This is converted into

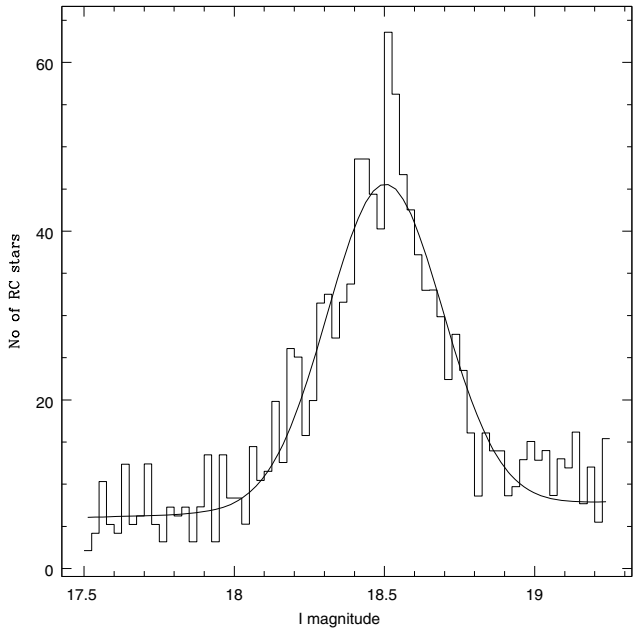

Fig. 6. A typical magnitude distribution of red clump stars in the SMC. The best fit to the distribution is also shown. The reduced χ^2 value of this fit is 1.36.

extinction in I band using the relation $A(I) = 0.934E(V-I)$, where $E(V-I)$ is the internal reddening estimated for each location. This was used to deconvolve the effect of internal extinction from the spread in magnitude. The above relation is derived from the relations $E(V-I) = 1.6E(B-V)$ and $A(I) = 0.482A(V)$ (Rieke & Lebofsky 1985). The interstellar extinction law of our Galaxy is adopted for the calculations of Magellanic Clouds based on the results of the studies by Nandy & Morgan (1978),

Lequeux et al. (1982) and Misslet et al. (1999), which showed that both LMC and SMC have extinction curves qualitatively similar to those found in Milky Way.

Thus, the net dispersion in magnitude due to depth alone was estimated for considered regions in the LMC and SMC. The resultant width in magnitude is converted into depth in kpc using the distance modulus formula and taking a distance of 50 kpc to the LMC and a distance of 60 kpc to the SMC.

The error in the estimation of the dispersion corresponding to depth is obtained from the errors involved in the estimation of width of colour and magnitude distribution. The random error associated with the width corresponding to depth is $\Delta\text{depth}^2 = \Delta I^2{}_{width} + \Delta(V-I)^2{}_{width}$. Thus the associated error in the estimation of depth is calculated for all the locations. This error will also translate as the minimum depth that can be estimated. The minimal depth that can be estimated is ~360 pc in the central regions of the LMC and ~650 pc in the outer regions of the LMC. In the SMC, the minimal thickness that can be estimated is ~350 pc in the central regions of the SMC and ~670 pc in the outer regions of the SMC.

5. Internal reddening in the MCs

One of the by products of this study is the estimation of internal reddening in the MCs. The shift of the peak of the $(V-I)$ colour distribution from the expected value was used by Subramaniam (2005) to estimate the line of sight reddening map to the OGLE II region of the LMC. The above study estimated the reddening between the observer and the observed region in the LMC. In this study, we used the width of the $(V-I)$ colour distribution to estimate the internal reddening map across the MCs. This estimates the front to back reddening of a given region in the MCs, which we call as the internal reddening (in $E(V-I)$), and does not estimate the reddening between the front end of the region and the observer. Thus, this estimate traces the reddening within the bar/disk of the MCs and hence the location of the dust. The estimates and figures given below thus gives the internal reddening within the MCs.

The colour coded figures of the internal reddening in the LMC and SMC are presented in Figs. 7 and 8 respectively. It can be seen that the internal reddening is high only in some specific regions in both the MCs. Most of the regions have very negligible internal reddening suggesting that most of the regions in the MCs are optically thin. The regions of high internal reddening in the LMC are located near the eastern end of the bar and the 30 Dor star forming region. The highest internal reddening estimated is $E(V-I) = 0.13$ mag in the OGLE II region of the LMC, which is the bar region and 0.16 mag in the MCPS region, close to the 30 Dor location. It is noteworthy that these are not very high values. The OGLE II internal reddening map shows that, apart from the eastern end of the bar, some regions near the center also have internal reddening. The MCPS data shows that the internal reddening across the LMC disk as seen by the RC stars is very small. The error associated with the width of colour distribution is translated as the minimum internal reddening that can be estimated. The minimum internal reddening that can be estimated in the central regions as well as in the disk of LMC is 0.003 mag. In the case of the SMC, a region of high internal reddening is found to the west of the optical center. Also, the bar region is found to have some internal reddening, whereas the disk has very little internal reddening (within the area studied). The highest reddening estimated is $E(V-I) = 0.08$ mag in the OGLE II regions and 0.12 mag in the MCPS region. These regions are located close to the optical center. The rest of the bar as well as the disk have very little internal reddening. Thus, our results indicate small extinction across the SMC, as seen by the RC stars. The minimum internal reddening that can be estimated is 0.002 mag in the central regions of SMC and 0.005 mag in the disk of SMC.

It is interesting to see low internal reddening across the MCs, as seen by the RC stars. This is in contradiction to the large extinction expected near the star forming regions, especially near 30 Dor. The reddening is estimated here using the same type of stars that are used to estimate the depth. Thus, we maintain the consistency of the same tracer for the above two properties. The higher values for the foreground reddening estimates were obtained by Harris et al. (1997) using the MCPS data for OB stars, whereas lower values were obtained using RC stars for the same regions by Subramaniam (2005) using OGLE II data. Thus, the reddening values estimated varied with respect to the tracer used. Once again, the present results confirm that the RC disk has much less internal extinction. This variation of reddening as a function of the population is suggestive of population segregation across the LMC. The above results suggest that the star forming regions in the LMC are likely to be behind the RC disk.

6. Results: the LMC

The line of sight depth in the LMC has been derived using two data sets. OGLE II data cover the central region and this is basically the bar region of the LMC. OGLE II data also cover a small detached disk region in the north-western direction. On the other hand, MCPS data cover a significant area of the disk, besides the bar. Thus the OGLE II data is suitable to derive the depth of the bar region, whereas the MCPS data is suitable to derive the depth of the bar as well as the disk regions. The two data sets can be used for consistency checks and the results derived will be compared.

The depth of 1528 regions of LMC (OGLE II data) were calculated. Out of 1528 regions, 1214 are in the central bar region and the remaining 314 regions are in the north western disk region. In the north western disk region there are regions with minimal thickness. The depth of 1301 regions of LMC (MCPS data) are also calculated. Regions with minimal thickness are seen in the disk of LMC.

A two dimensional plot of the depth for the 1528 OGLE II regions is shown in the lower panel of Fig. 9. This plot is colour coded as explained. The optical center of the LMC is taken to be RA = $05^h19^m38^s$, Dec = –69°27′5.″2 (J2000.0, de Vaucoulers & Freeman 1973). The OGLE II data show a range of dispersion values from 0.03 to 0.46 mag (a depth of of 690 pc to 10.5 kpc; avg: 3.95 ± 1.42 kpc) for the LMC central bar region. For the N-W disk region, the dispersion estimated ranges from 0.023 mag to 0.33 mag (a depth of 500 pc to 7.7 kpc; avg: 3.56 ± 1.04 kpc).The minimum value in the N-W disk region is limited by errors. The fraction of such regions, where the minimum value is limited by errors, is 4.06%. Regions in the bar between RA 80–84 degrees show a reduced depth (0.5–4 kpc, as indicated by yellow and black points). The regions to the east and west of the above region are found to have larger depth (2.0–8.0 kpc, black, red and green points). Thus, the depth of the bar at its ends is greater than that near its center. Since the center of the bar does not coincide with the optical center, the thinner central bar region is located to the east of the optical center. The average values of these three regions of the bar are 3.21 ± 1.03 kpc for the central minimum, 4.13 ± 1.35 kpc for the western region and 4.95 ± 1.49 kpc for the eastern region. This is better brought out in Fig. 10, where the depth is shown

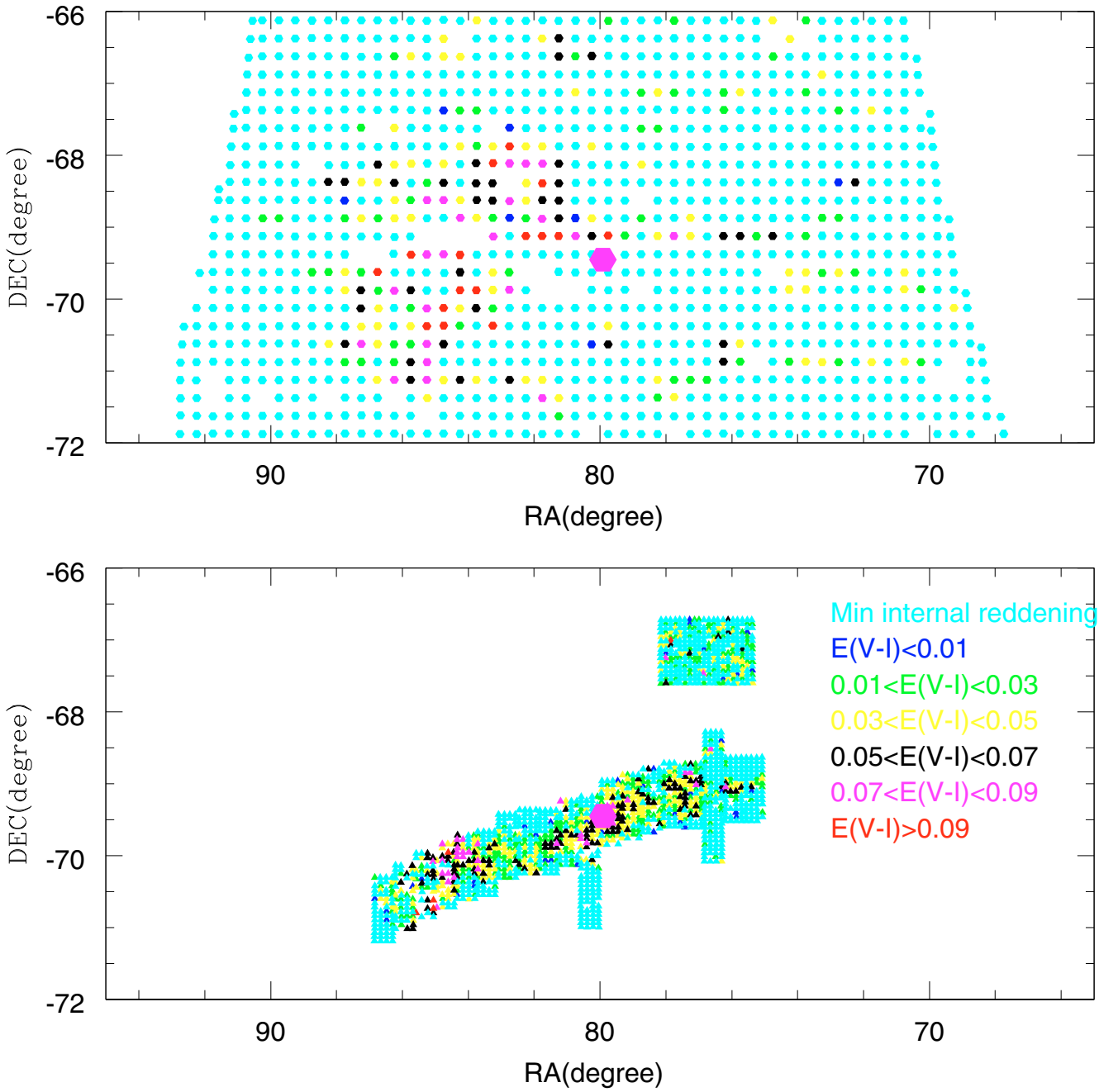

Fig. 7. Two dimensional plot of the internal reddening in the LMC. The colour code is given in the figure. The magenta dot represents the optical center of the LMC. The upper plot is derived from the MCPS data, whereas the lower plot is derived from the OGLE II data.

as a function of RA (the Dec range in OGLE II data is less when compared to the RA range). The lower panel shows the bar region and the upper panel shows the N-W disk region. An indication of flaring is seen here. In this figure, the depth of all the regions are shown and the error bar on each point denotes the error in the estimation of depth at each location. The depth averaged along the Dec of each RA is shown in Fig. 12. This plot clearly suggests that the bar is flared at its ends. The open circles indicate the N-W disk points. Thus the N-W region has a depth similar to the central region of the bar. The plot also suggests that the eastern end of the bar is more flared than the western end. The errors shown are the standard deviation of the average, thus a large error indicates a large range in the depth values.

We also used the MCPS data to estimate the depth in the bar region. This data set could not be corrected for data incompleteness and thus might underestimate the RC stars, especially in the crowded bar region. This is also reflected in the number counts, since a larger area is required to obtain a similar number of red clump stars. We used larger area bins for the MCPS data and estimated the depth. The colour-coded figure for the LMC (bar and the disk) is shown in the upper panel of Fig. 9. A prominent feature of the plot is the lop-sided distribution of the red dots (greater depth) when compared to the black dots (lesser depth). Thus, this plot reveals that there is a variation in depth across the disk of the LMC. The average depth for the bar estimated based on 320 regions is 4.3 ± 1.0 kpc, which is very similar to the value estimated from the OGLE II data. The large dispersion is not due to errors in the estimation of the depth of individual regions, but is due to the presence of regions with varying depths in the bar region.

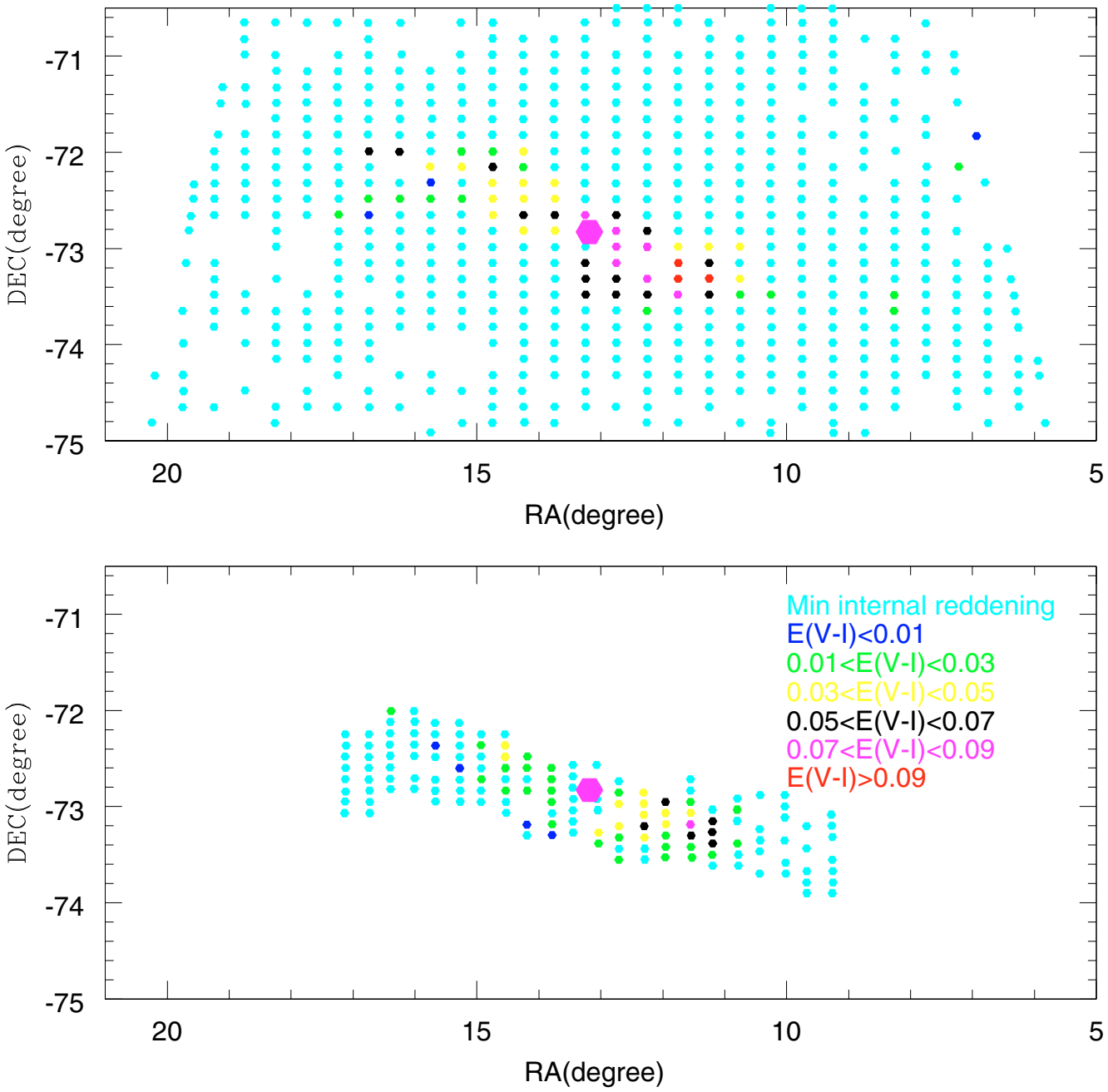

Fig. 8. Two dimensional plot of the internal reddening in the SMC. The colour code is given in the figure. The magenta dot represents the optical center of the SMC. The upper plot is derived from the MCPS data, whereas the lower plot is derived from the OGLE II data.

We used the MCPS data to estimate the depth of the disk. We considered regions outside the location of the bar as disk regions. The estimated depth ranges from 650 pc to 7.01 kpc.The minimum value of depth is limited by errors. The fraction of such regions, where the minimum value is limited by errors, is 0.44%. The average of the disk alone is estimated to be 3.44 ± 1.16 kpc. The average values of the depth for different disk regions were estimated and are tabulated in Table 1, along with the values for the bar for comparison. It can be seen that the average depth of the northern disk is greater than the southern disk by more than 2σ (of the southern disk). The depth of the northern disk is similar to the depth estimated for the bar. Thus the bar and the northern disk of the LMC have greater line of sight depth, whereas the east, west and the southern disk have reduced depth. The variation of depth as a function of RA (bottom panel) and Dec (top panel) is shown in Fig. 11. The depth variation as a function of RA indicates that the east and the west ends have a depth less than the bar, whereas the depth variation as a function of Dec indicates that the depth reduces from north to the south disk, with increased depth in the bar regions. The fact that the northern disk of the LMC has a greater depth compared to the other regions seems to be a surprising result. It will be interesting to study the line of sight depth of regions located further north, to find out how far this trend continues in the disk. Figure 9 (upper panel) also gives a mild suggestion that the depth of the disk gradually reduces towards the south, especially on the south-western side. This is indicated by the increase of yellow points and the appearance of cyan points. The plot also mildly suggests that the maximum gradient in the depth is seen from the north-east to the south west of the LMC disk. This is similar to the position angle

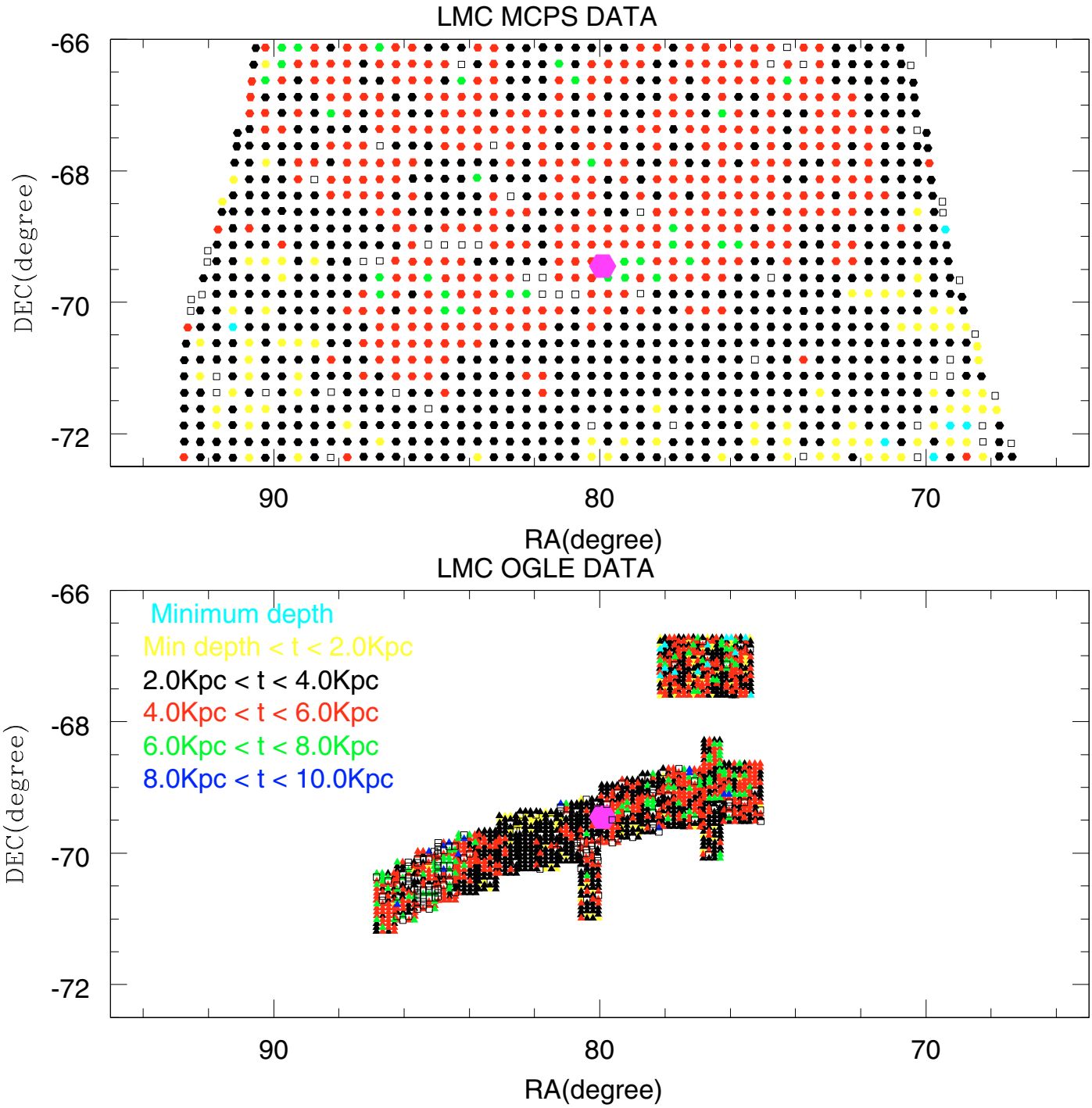

Fig. 9. Two dimensional plot of depth (t) in the LMC. The colour code is given in the figure. The magenta dot represents the optical center of the LMC. The empty squares represent the omitted regions with poor fit.

of the minor axis of the LMC (major axis ~120°, van der Marel et al. 2002). Within the radius of the disk studied here, there is no evidence for flaring of the disk. An estimation of depth of outer disk at large radii is essential to confirm the above indicated trends.

7. Results: the SMC

In the case of the SMC also, we used OGLE II and MCPS data sets. Similar to the LMC, the area covered by OGLE II is mainly the bar region, whereas the bar and disk are covered by the MCPS data. The depth of 150 regions (OGLE II data) and 600 regions (MCPS data) of the SMC were calculated.

A colour coded, two dimensional plot of depth for these two data sets are shown in Fig. 13 (OGLE II data in the lower panel and MCPS data in the upper panel). The optical center of the SMC is taken to be RA = $00^{h}52^{m}12.5^{s}$, Dec = –72°49′43″ (J2000, de Vaucoulers & Freeman 1973). There is no indication of a variation of depth across the disk as indicated by the uniform distribution of the red and black dots. The prominent feature in both the plots is the presence of blue and green points indicating increased depth, for regions located near the SMC optical

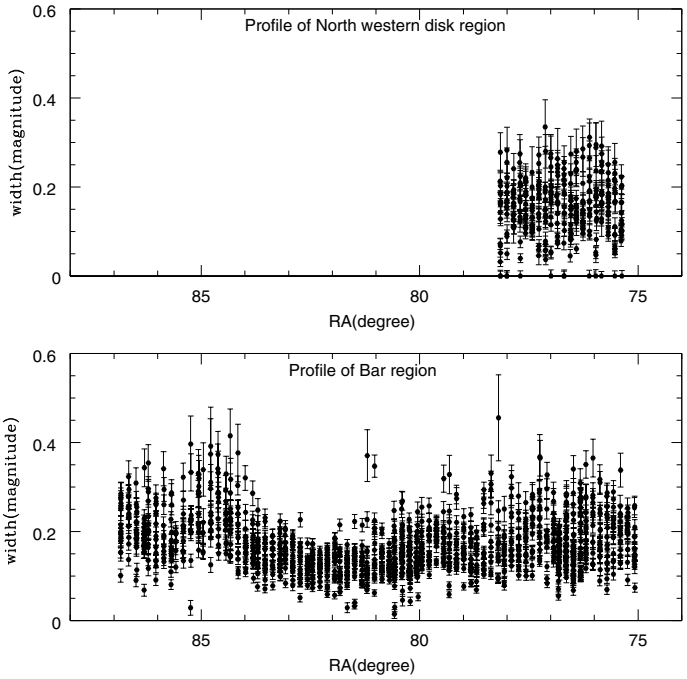

Fig. 10. Width corresponding to depth with error bars plotted against RA for both the central bar region and north western disk region of LMC.

center. The OGLE II data cover only the bar region and it can be seen that this data is not adequate to identify the extension of the central feature, whereas the MCPS data clearly delineates this feature.

The net dispersions range from 0.10 to 0.35 mag (a depth of 2.8 kpc to 9.6 kpc) in the OGLE II data set and from 0.025 mag to 0.34 mag (a depth of 670 pc to 9.47 kpc) in the MCPS data set. The minimum depth estimated in the MCPS data is limited by errors. The fraction of such regions where the minimum value is limited by errors is 2.83%. The average value of the SMC thickness estimated using the OGLE II data set in the central bar region is 4.9 ± 1.2 kpc and the average thickness estimated using MCPS data set, which covers a larger area than OGLE II data, is 4.42 ± 1.46 kpc. The average depth obtained for the bar region alone is 4.97 ± 1.28 kpc, which is very similar to the value obtained from OGLE II data. The depth estimated for the disk alone is 4.23 ± 1.47 kpc. Thus the disk and the bar of the SMC do not show any significant difference in the depth. The marginal difference between the bar and the disk depths is due to the presence of higher depth regions near the center. Thus, except for the central feature, the depth across the SMC appears uniform. Our estimate is in good agreement with the depth estimate of the SMC using eclipsing binary stars by North et al. (2008). They estimated a 2-sigma depth of 10.6 kpc, which corresponds to a 1-sigma depth of 5.3 kpc.

In order to study the variation of depth of the SMC (OGLE II data) along the RA, dispersion corresponding to the depth is plotted against RA in Fig. 14. The lower panel shows all the regions along with the error in depth estimation for each location. The upper panel shows the depth averaged along Dec and the error indicates the standard deviation of the average. Both the panels clearly show the increased depth near the SMC center. There is no significant variation of depth along the bar.

For MCPS data, the dispersion corresponding to depth is plotted against RA as well as DEC in Fig. 15. There is an indication of increased depth near the center, as seen before. The plot also indicates that there is no significant variation in depth between the bar and the disk, and there is no indication of variation of depth across the disk. In Fig. 16, the depth averaged over RA and Dec are shown in the upper and lower panel respectively. These are plotted for a small range of Dec (−72.0–−73.8 degrees) and RA (10–15 degrees), in order to identify the increased depth in the central region. The increased depth near the center is clearly indicated. Thus, the depth near the center is about 9.6 kpc, which is twice the average depth of the bar region (4.9 kpc). Thus, the SMC has a more or less uniform depth of 4.9 ± 1.2 kpc over bar as well as the disk region, with double the depth near the center.

8. Discussion

The line of sight depth of MCs are estimated using red clump stars as tracers. They are intermediate age stars with ages greater than 1 Gyr, hence, the depth estimates correspond to the intermediate age disk. The depth of the intermediate age disk may give clues to its evolution, as a thin disk is indicative of an undisturbed disk, whereas a thick disk would indicate a heated up and hence disturbed disk. Thus the depth of the disks as well as the bar regions of these galaxies are clues to the evolution of these galaxies. The analysis presented here estimates the dispersion in the RC magnitude distribution due to depth, after correcting for dispersion due to other effects. The corrections due to the internal reddening and observational error were estimated for each region and were corrected accordingly. The correction for the presence of an age and metallicity range in the RC population, along with star formation history is done using the dispersion estimated by Girardi & Salaris (2001). Thus the values estimated here have a bearing on the assumptions made during the correction of the above effect.

The variation in the estimated dispersion (after all the corrections) is assumed to be due to variations in depth across the galaxy. If this is actually due to the differences in RC population, as a result of variation in age, metallicity and star formation history, then the results indicate that the RC population and their properties are significantly different in the bar, north and south of the disk, for the LMC. Recent studies show that the above parameters are more or less similar across the LMC (Subramaniam & Anupama 2002; Olsen & Salyk 2002; van der Marel & Cioni 2001). Variation of star formation history and metallicity across the LMC has been studied by Cioni et al. (2006b), Carrera et al. (2008). They found small variations in the inner regions, but large variations in the outer regions. Cioni et al. (2006b) mapped the variation of star formation history as well as metallicity using the AGB stars. They found that the south and south-western regions could be metal poor whereas the north and north-eastern regions could be metal rich. Regions near the Shapley constellation III were found to have a younger population. This region is close to the northern limit studied here. Piatti et al. (1999) and Dolphin (2000) found that the RC population in the far northern regions is structured. All the above regions with varying RC population are outside the regions studied here. The results presented in this study suggests that the northern regions and the bar have large dispersion, probably due to depth when compared to the east, west and the southern regions. If this is not due to increased depth in these regions, then it would mean that the stellar populations in these regions are significantly different. In either case, the northern disk and the bar seem to be different from the rest of the LMC disk.

As incompleteness correction is done in one data set (OGLE II) and not in the other (MCPS) we compared the depth

Table 1. Depths of different regions in the LMC & SMC. These are line of sight depths and need to be corrected for inclination, to estimate the actual depth.

Region	Range of depth (kpc)	Avg. depth (kpc)	Std. deviation (kpc)
LMC eastern bar (RA > 84.°0)	0.69–9.10	4.95	1.49
LMC western bar (RA < 80.°0)	1.26–10.44	4.14	1.35
LMC central bar (80.°0 < RA < 84.°0)	0.69–8.50	3.21	1.03
LMC bar average	0.69–10.44	3.95	1.42
LMC eastern disk (RA > 88.°0, −68.°0 > Dec > −71.°0)	0.65–5.89	2.80	0.92
LMC western disk (RA < 74.°0, −68.°0 > Dec > −71.°0)	0.65–5.58	3.08	0.99
LMC northern disk (Dec > −68.°0)	1.00–7.01	4.17	0.97
LMC southern disk (Dec < −71.°0)	0.65–4.58	2.63	0.79
LMC disk average	0.65–7.01	3.44	1.16
SMC bar	3.07–9.53	4.90	1.23
SMC disk	0.67–9.16	4.23	1.48

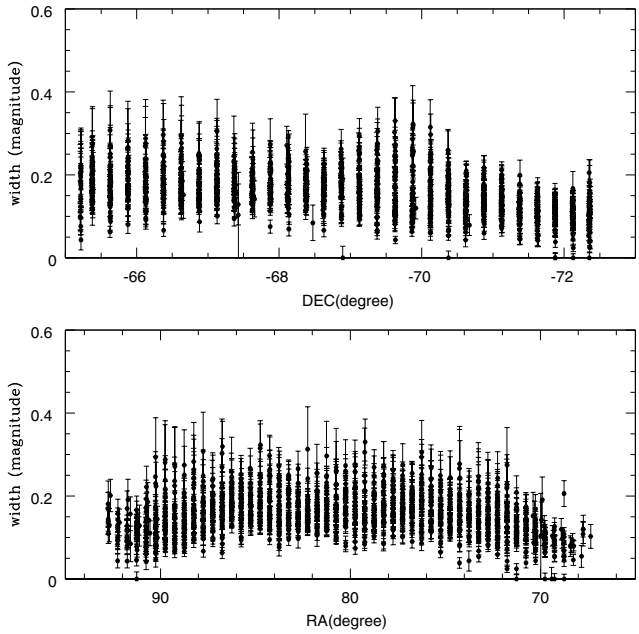

Fig. 11. Width corresponding to depth with error bars plotted against RA and Dec for the LMC MCPS data.

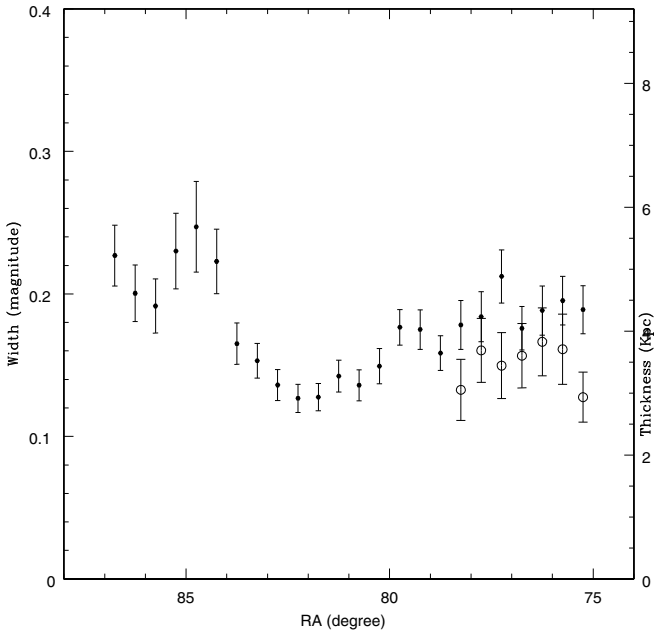

Fig. 12. Width corresponding to depth averaged along the declination plotted against RA for both the central bar region (closed circles) and north western disk region (open circles) of LMC.

estimates before and after adopting the completeness correction. We found that the change is within the bin sizes adopted here. Thus, incorporating the incompleteness correction has not changed the results presented here. The incompleteness correction is large in the central regions of the LMC bar, where the correction is between 30–40 percent. The outer regions of the bar (6–15%) as well as the NW region (5–9%) have less correction. The outer regions are thus less affected by the incompleteness. Thus the incompleteness problem is unlikely to affect the MCPS RC distribution in the LMC disk, whereas it may be unreliable in the central regions of the LMC bar. In the SMC, the incompleteness correction in the central regions is about 12% and that in the outer region is about 5%. This is the case for SMC also. The incompleteness in the MCPS data does not affect the results presented here.

We have removed regions in the MCs with poor fit as explained in section 4. These regions are likely to have different RC structures suggesting a large variation in metallicity and/or population. The fraction of such regions is about 8% in the LMC and 5.3% in the SMC. Such regions are indicated in Figs. 9 and 11. Thus to a certain extent, the above procedure has eliminated the regions with very different metallicity and star formation history that are seen in most of the regions. Apart from the above, the remaining regions studied here might have some variation in the the RC population contributing to the depth estimated. The results presented in this study will include some contribution from the population effect.

The estimated depth for various regions in the LMC is given in Table 1. These values correspond to the 1-sigma depth. In the case of the LMC, the line of sight depth estimated here is for the inclined disk. To estimate the actual depth of the disk, one needs to correct for the inclination. Assuming the inclination to be 35 degrees (van der Marel et al. 2001), the actual depth of the bar is $4.0 \times \cos(i) = 3.3 \pm 1.0$ kpc. Similarly, the southern disk has an actual depth of about 2.2 ± 1.0 kpc, whereas the northern disk is similar to the bar. Note that, after correcting for inclination, the depths in the northern and the souther regions are within the errors. This is because the difference in depth reduces due to correction for inclination, but the error does not. These values should be used when one compares the depth of the LMC with that of other galaxies. Thus, the LMC bar and the disk are

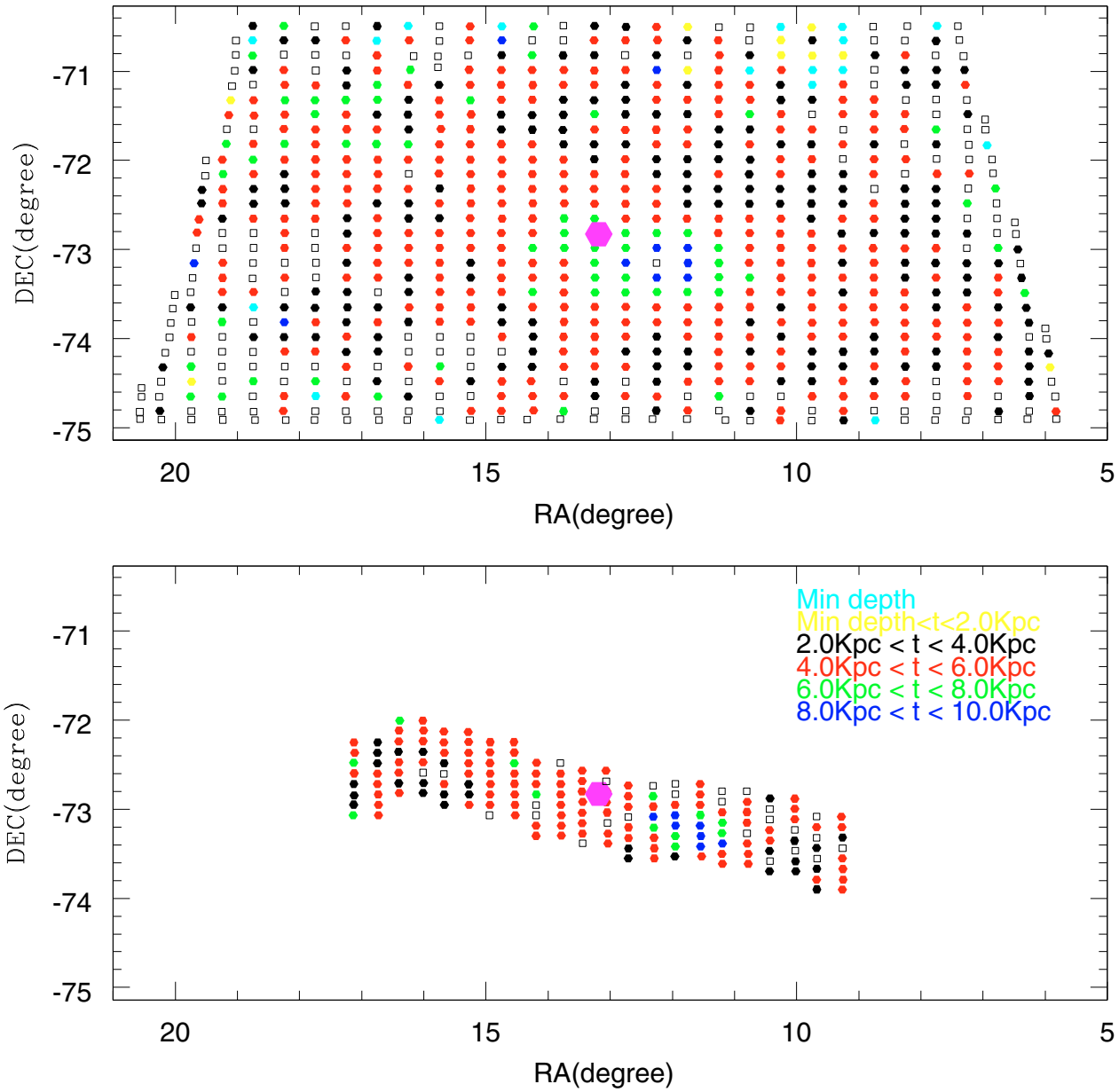

Fig. 13. Two dimensional plot of depth (t) in the SMC. *Upper panel* is for the MCPS data and *lower panel* is for OGLE II data.The colour code is same for both the panels. The magenta dot represents the optical center of the SMC. The empty squares represent the omitted regions with poor fit.

thicker than the thin disk of our Galaxy (~100 pc). The scale height of the bar could be taken as half of its depth, assuming that the bar is optically thin. The z-extent of the bar, which is the scale height (1.65 kpc), is found to be similar to its scale length (1.3–1.5 kpc, van der Marel 2001). Hence the bar has a depth similar to its width. Thus the bar continues to be an unexplained structure/component of the LMC.

The LMC bar is found to be fairly thick (line of sight depth = 4.0 ± 1.4 kpc). We also find evidence for flaring and a disturbed structure at the ends of the bar region. The thick and flared bar of the LMC indicates that this region of the LMC is perturbed. The structure of the LMC bar as delineated by the RC stars showed warps (Subramaniam 2003), which is also clear indication of disturbance. The depth estimates also suggest that the LMC disk is fairly thick (2.4–4.0 kpc), with a decrease in depth/thickness and/or varying stellar population from the north to the south. The tidal effects due to LMC-Galaxy interactions (if they were interacting) are unlikely to cause this, as the tidal effects are stronger near the outer regions and weaker towards the inner regions. Flaring of the disk is expected if tidal interactions are present. On the other hand, except for the thicker northern region, flaring of the disk is not seen, at least up to the radii studied here. Hence we do not see any evidence for tidal interactions, at least in the inner disk. The recent results on the proper motion of the LMC and SMC (Kallivayalil et al. 2006a) suggested that the Clouds are approaching our Galaxy for the first time. This would suggest that the LMC has not interacted with our Galaxy before. Our results are in good agreement with this scenario.

In general, thicker and heated up disks are considered as signatures of minor mergers (Quinn & Goodman 1986; Velazquez & White 1999). Thus, the LMC is likely to have experienced minor mergers in its history. The presence of warps in the bar (Subramaniam 2003) and evidence of counter rotation in the central regions (Subramaniam & Prabhu 2005) also support the minor merger scenario. Thus, it is possible that the LMC has

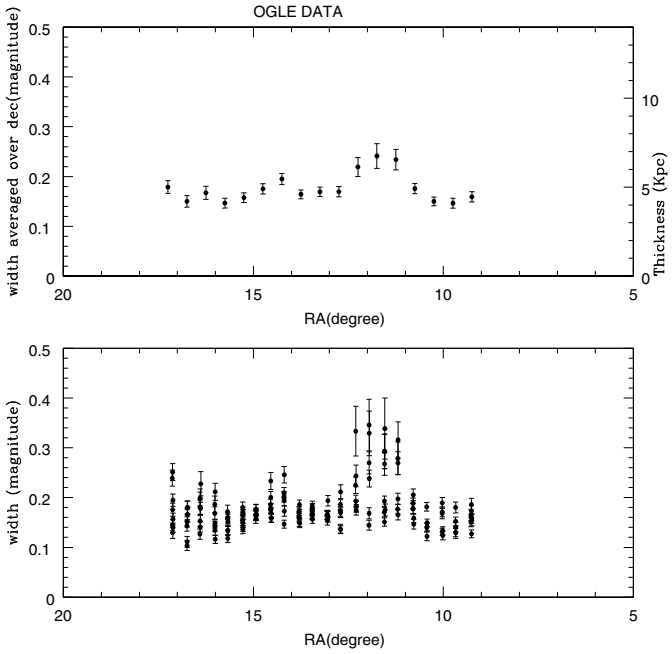

Fig. 14. *Lower panel*: width corresponding to depth against RA for bar region of the SMC (OGLE II data). *Upper panel*: average of depth along the declination against RA in the bar region of the SMC (OGLE II data).

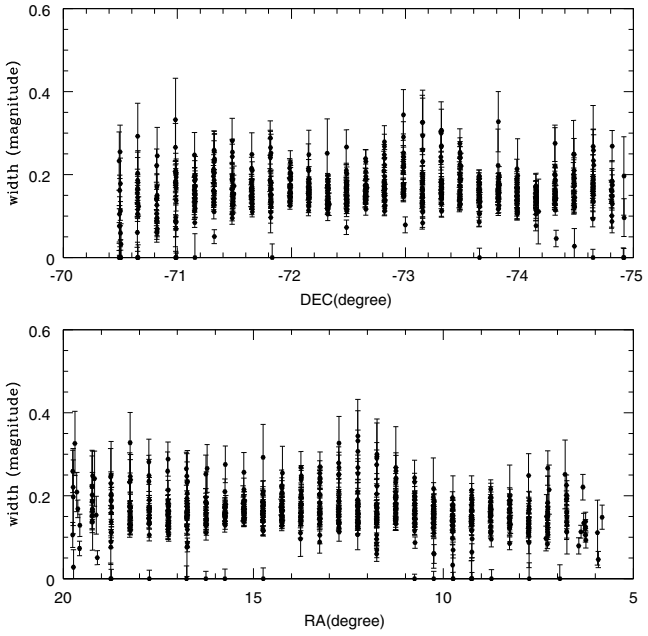

Fig. 15. Width corresponding to depth against RA in the *lower panel* and against Dec in *the upper panel* for the SMC (MCPS data).

experienced minor mergers during its evolution. These mergers have affected the northern disk and the bar. The variation in depth observed across the LMC disk could constrain the way in which these mergers could have happened.

The SMC is found to have a depth greater than the LMC. The disk and the bar does not show much difference in depth. A striking result is the increased depth in the central region of the SMC. The profile of the depth near the center (Fig. 16) looks very similar to a typical luminosity profile of a bulge. This could

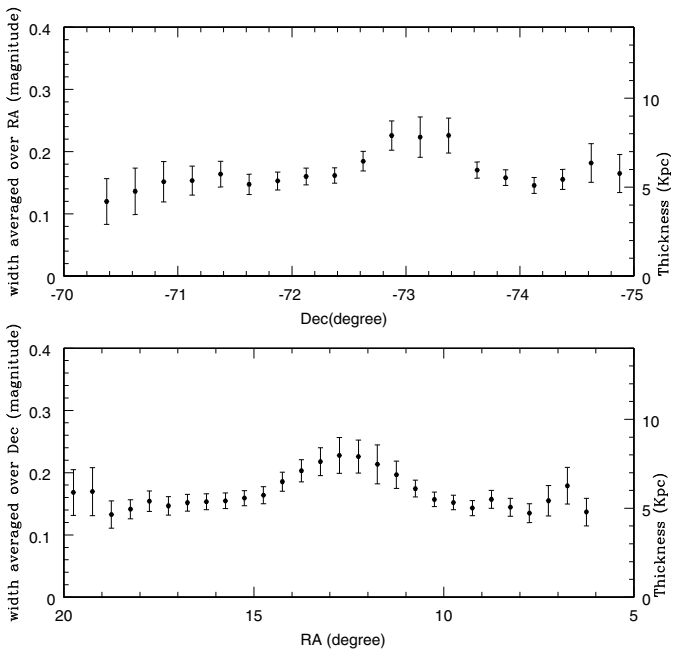

Fig. 16. *Lower panel*: width corresponding to depth averaged over Dec and plotted against RA for a small range of Dec in the central region of the SMC (MCPS data). *Upper panel*: width corresponding to depth averaged over RA and plotted against Dec for a small range of RA in the central region of the SMC (MCPS data).

suggest the presence of a bulge near the optical center of the SMC. If a bulge is present, then a density/luminosity enhancement in this region is also expected. We plotted the observed stellar density in each region from the MCPS data to see whether there is any such central enhancement. This is shown in Fig. 17. The regions with high density are shown as open circles, located close to the optical center. The regions with large depth are found to be within the ellipse shown in the figure. It can be seen that regions with highest stellar density lie more or less within this ellipse. Cioni et al. (2000) studied the morphology of the SMC using the DENIS catalogue. They found that the distribution of AGB and RGB stars show two central concentrations, near the optical center, which match with the carbon stars by Hardy et al. (1989). They also found that the western concentration is dominated by old stars. The approximate locations of these two concentrations found by Cioni et al. (2000) are shown as hexagons in Fig. 17. Also, the strongest HI concentration in the SMC map by Stanimirovic et al. (1999) falls between these two concentrations. The maximum HI column density, 1.43×10^{22} atoms cm^{-2} is located at RA = $00^{h}47^{m}33^{s}$, Dec = –73°05′26″ (J2000.0) (Stanimirovic et al. 2004). This location is shown as a large triangle in Fig. 17. The optical center of the SMC is shown as a large square. All these peaks as well as the optical center are located on or within the boundary of the ellipse. Thus, the peaks of stellar as well as the HI density are found within the central region with large depth. This supports the idea that a bulge may be present in the central SMC. This bulge is not very luminous, but clearly shows enhanced density. It is also the central region of the triangular shaped bar.

The increased dispersion near the SMC center, which is interpreted as due to large depth, could be partially due to the presence of RC population which is different. Cioni et al. (2006a) did not find any different population or metallcity gradient near the central regions. Tosi et al. (2008) obtained deep CMDs of

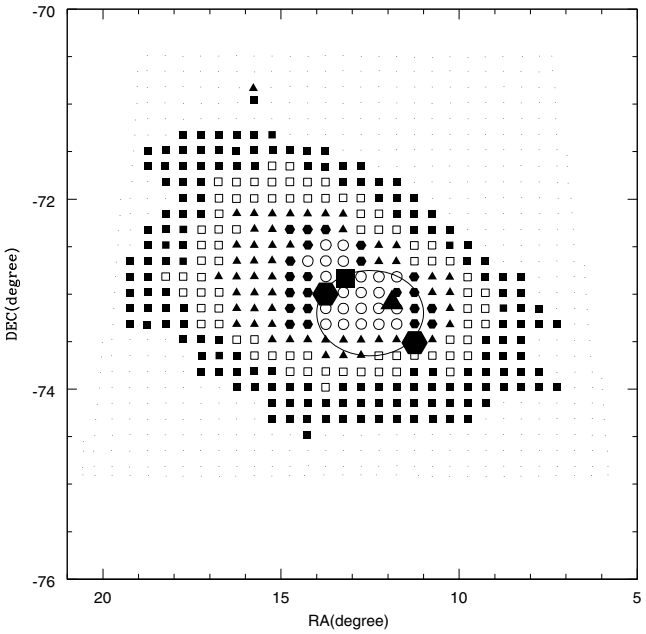

Fig. 17. Two dimensional plot of density distribution estimated from MCPS data. The small open circles in the central region indicate the high density regions. The ellipse shows the boundary of regions with large depth, the large hexagons indicate the stellar peaks found by Cioni et al. (2000), the large triangle indicate the HI peak (Stanimirovic et al. 2004) and the large square denotes the optical center.

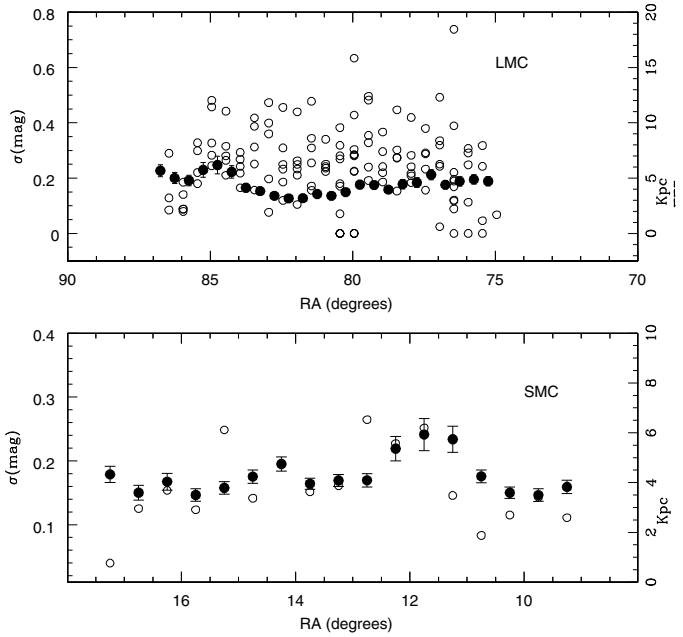

Fig. 18. *Lower panel*: width corresponding to depth estimated from RR-Lyrae (open circles) and from red clump stars (closed circles) is plotted against RA for the SMC. Theupper panel shows a similar plot for the LMC.

6 SMC regions to study the star formation history. Three of their regions are located close to the bar and three are outside the bar. They found an apparent homogeinty of the old stellar population populating the subgiant branch and the clump. This suggested that there is no large differences in age and metallicity among old stars in these locations. Their SF1 region is located close to the region of large depth identified here. The RC population in this region is found to be very rich and the spread in magnitude is greater than those found in the other CMDs. This spread is also suggestive of increased depth near this location. It will be worthwhile to study the star formation history of regions near the SMC center to understand how different the stellar population is in this suggested bulge.

It may be worthwhile to see whether this bar is actually an extended/deformed bulge. It is interesting that the so-called triangular shaped bar of the SMC is also an unexplained component, which does not show the signatures of a typical bar. This could naturally explain the formation of the odd shaped bar in the SMC. Thus, we propose that the central SMC has a bulge. The elongation and the rather non-spherical appearance of the bulge could be due to tidal effects or minor mergers (Bekki & Chiba 2008).

9. Disk and halo of the LMC

Subramaniam (2006) studied the distribution of RR Lyrae stars in the bar region of the LMC. She found that the RR Lyrae stars in the bar region have a disk-like distribution, but halo-like location. The RR Lyrae stars are in the same evolutionary state as the RC stars, except that the RR Lyrae stars belong to an older and metal poor population. Therefore they are good tracers of the halo. Thus, it will be interesting to compare the depth of the halo as defined by the RR Lyrae stars and the depth of the disk as defined by the RC stars.

Subramaniam (2006) derived the dispersion in the extinction corrected average I magnitude of RR Lyrae stars in the bar region. After correcting for contribution to the dispersion due to other factors, the dispersion due to depth was estimated. The total depth estimated for RR Lyrae stars in this paper was compared with the RC depth. The upper panel of Fig. 18 shows the dispersion as estimated from RR Lyrae stars as open circles and that estimated average from RC stars as dots. The figure shows that the RR Lyrae depth ranged between 4.0 and 8.0 kpc (corresponding to a scale height of 2.0–4.0 kpc, as reported in the above paper). Since the RR Lyrae stars were studied in the bar region, this comparison is valid only for the bar region. It is assumed that the bar is part of the disk, and hence allowing the comparison of disk vs halo. It can be seen that the depth as indicated by the RC stars is approximately the lower limit set by the RR Lyrae stars. That is, the RR Lyrae stars span a greater depth than the RC stars. Thus, at least in the central region of the LMC, the halo, as delineated by the RR Lyrae stars, has a much greater depth than the disk, as delineated by the RC stars. This supports the idea that there is an inner halo for the LMC. It is interesting that, in an outside-in collapse scenario, the disk starts to form at the end of the halo formation. This transition is more or less indicated in the figure as the transition where the RR Lyrae stars stop forming in the halo and the RC stars take over and the disk forms. In order to make this statement conclusive, we need to make such a comparison for the entire disk region of the LMC, not just the bar region. The present study, though indicative, suggests that the halo to disk transition of the LMC follows the outside-in formation, at least in the inner regions.

10. Disk and halo of the SMC

A similar comparison can be made between the halo and disk/bar of the SMC. The RR Lyrae stars from the OGLE II data were analysed similarly to the procedure adopted by Subramaniam (2006). The depth along the line of sight is estimated from the observed dispersion in the extinction-corrected mean I magnitude of 458 ab type RR Lyrae stars. The dispersion due to depth alone was estimated after correcting for the metallicity and evolutionary effects. These were compared with the dispersion estimated from RC stars in the lower panel of Fig. 18. It can be seen that, contrary to what is seen in the case of the LMC, both populations show a very similar dispersion in the SMC. The figure not only suggests that the RR Lyrae stars and the RC stars occupy a similar depth, but also indicates that they show a similar depth profile across the bar. The increased depth near the optical center is also closely matched. This suggests that the RR Lyrae stars and RC stars are born in the same location and occupy a similar volume in the galaxy. This is a puzzling combination, as in general, the RR Lyrae stars and RC stars do not co-exits, as they belong to the halo and disk population respectively.

On the other hand, there is one location in the galaxy where this can take place, which is the bulge. That is, we do see the very metal-poor low mass stars (RR Lyrae stars) and the higher mass metal rich counter parts (RC stars) co-existing in the bulge. Thus, the co-existence and the similar depth of RR Lyrae stars and the RC stars in the central region of the SMC can be easily explained, if it is the bulge. Thus the bar region of the SMC could in fact be a bulge. This is in good agreement with the result obtained earlier, where a bulge-like depth, and enhanced stellar and HI density were found near the optical center. If this is true, then most of the RR Lyrae stars in the central region belong to this bulge and not the halo. The depth of both these populations in the outer regions need to be compared to make this picture complete.

Thus, the formation and evolution of the two clouds do not seem to be similar. The LMC is more or less an irregular galaxy with a disk. On the other hand, the SMC could be a spheroid. In this study we propose that the SMC has a bulge and the so-called bar is possibly this deformed/extended bulge. The LMC does not have a bulge, but, the SMC has managed to form a bulge. The LMC seems to have undergone minor mergers, whereas the SMC seems to have experienced tidal forces and/or minor mergers. The structure of the inner LMC agrees well with the outside-in formation of the LMC. We do not find any evidence for such an inner halo in the SMC. Thus, even though the clouds are located close to each other now, the early formation and evolution of these two galaxies appear different.

11. Conclusions

1) The LMC and the SMC are found to have large line of sight depths (1-sigma) for the bar (4.0 ± 1.4 and 4.9 ± 1.2 kpc) and disk (3.44 ± 1.16 kpc and 4.23 ± 1.48 kpc).
2) The LMC bar(4.0 ± 1.4 kpc) and the northern disk (4.17 ± 0.97 kpc) have similar, but large depth. The eastern (2.8 ± 0.92 kpc), western (3.08 ± 0.99 kpc) and the southern (2.63 ± 0.79 kpc) disk have similar, but reduced depth. This may also be interpreted as due to different stellar populations.
3) The depth profile indicates flaring of the LMC bar.
4) The LMC halo is found to have greater depth than the disk/bar, which supports the presence of the inner halo for the LMC. The structure of the inner LMC agrees well with the outside-in formation of the LMC.
5) The SMC bar and the disk have similar depth, with no significant depth variation across the disk.
6) Increased depth is found near the optical center of the SMC.
7) The co-existence of RR Lyrae stars and RC stars in the central volume, along with the increased depth and stellar & HI density near the center, suggest that the SMC possibly has a bulge. The central bar may be this deformed/extended bulge.
8) The large depths of the L&SMC suggest that they have experienced heating, probably due to minor mergers.

Acknowledgements. We thank the anonymous referee for the encouraging comments which improved the presentation of the paper.

References

Alves, D. R., & Nelson, C. A. 2000, ApJ, 542, 789
Bekki, K., & Chiba, M. 2008, ApJ, 679, L89
Besla, G., Kallivayalil, N., Hernquist, L., et al. 2007, ApJ, 668, 949
Carrera, R., Gallart, C., Hardy, E., et al. 2008, AJ, 135, 836
Cioni, M.-R. L., Habing, H. J., & Israel, F. P. 2000, A&A, 358, L9
Cioni, M.-R. L., Girardi, L., Marigo, P., & Habing, H. J. 2006a, A&A, 452, 195
Cioni, M.-R. L., Girardi, L., Marigo, P., & Habing, H. J. 2006b, A&A, 448, 77
de Vaucouleurs, G., & Freeman, K. C. 1973, Vistas Astron., 14, 163
Dolphin, A. E. 2000, MNRAS, 313, 281
Girardi, L., & Salaris, M. 2001, MNRAS, 323, 109
Hardy, E., Suntzeff, N. B., & Azzopardi, M. 1989, AJ, 344, 210
Harris, J., Zaritsky, D., & Thompson, I. B. 1997, AJ, 114, 1933
Hatzidimitriou, D., & Hawkins, M. R. S. 1989, MNRAS, 241, 667
Holtzman, J. A., Gallagher, J. S. III., Cole, A. A., et al. 1999, AJ, 118, 2262
Kallivayalil, N., van der Marel, R. P., Alcock, C., et al. 2006a, ApJ, 638, 772
Kallivayalil, N., van der Marel, R. P., Alcock, C., et al. 2006b, ApJ, 652, 1213
Lequeux, J., Maurice, E., Prevot-Burnichon, M.-L., et al. 1982, A&A, 113, L15
Mathewson, D. S., Ford, V. L., & Visvanathan, N. 1986, ApJ, 301, 664
Mathewson, D. S., Ford, V. L., & Visvanathan, N. 1988, ApJ, 333, 617
Misselt, K. A., Clayton, G. C., & Gordon, K. D. 1999, ApJ, 515, 128
Nandy, K., & Morgan, D. H. 1978, Nature, 276, 478
North, P. L., Gauderon, R., & Royer, F. 2008 [arXiv:0809.2728]
Olsen, K. A. G., & Salyk, C. 2002, AJ, 124, 2045
Paczynski, B., & Stanek, K. Z. 1998, ApJ, 494, L219
Pagel B. E. J., & Tautvaisiene, G. 1998, MNRAS, 299, 535
Piatti, A. E., Geisler, D., Bica, E., et al. 1999, AJ, 118, 2865
Quinn, P. J., & Goodman, J. 1986, ApJ, 309, 472
Rieke, G. H., & Lebofsky, M. J. 1985, ApJ, 288, 618
Stanimirovic, S., Staveley-Smith, L., & Dickey, J. M. 1999, MNRAS, 302, 417
Stanimirovic, S., Staveley-Smith, L., & Jones, P. A. 2004, ApJ, 604, 176
Subramaniam, A. 2003, ApJ, 598, L19
Subramaniam, A. 2005, A&A, 430, 421
Subramaniam, A. 2006, A&A, 449, 101
Subramaniam, A., & Anupama, G. C. 2002, A&A, 390, 449
Subramaniam, A., & Prabhu, T. P. 2005, ApJ, 625, L47
Szymanski, M. 2005, Acta Astron., 55, 43
Tosi, M., Gallagher, J., Sabbi, E., et al. 2008 [arXiv:0808.1182]
Udalski, Kubiak & Szymanski 1997, Acta Astron., 47, 319
Udalski, A., Szymanski, M., Kubiak, M., et al. 1998, Acta Astron., 48,147 (SMC OGLE II data)
Udalski, A., Szymanski, M., Kubiak, M., et al. 2000, Acta Astron., 50, 307 (LMC OGLE II data)
van der Marel, R. P. 2001, AJ, 122, 1827
van der Marel, R. P., & Cioni, M. L. 2001, AJ, 122, 1807
van der Marel, R. P., Alves, D. R., Hardy, E., et al. 2002, AJ, 124, 2639
Velazquez, H., & White, S. D. M. 1999, MNRAS, 304, 254
Welch, D. L., McLaren, R. A., Madore, B. F., et al. 1987, ApJ, 321, 162
Weinberg, M. D. 2000, ApJ, 532, 922
Westerlund, B. E. 1997, The Magellanic Clouds (Cambridge: Cambridge Univ. Press)
Zaritsky, D., Harris, J., Thompson, I. B., et al. 2002, AJ, 123, 855 (SMC MCPS data)
Zaritsky, D., Harris, J., Thompson, I. B., et al. 2004, AJ, 128, 1606 (LMC MCPS data)